TITLE: Laminar Design for Supersonic Civil Transport

Laminar Design for Supersonic Civil Transport

Achmed Traoré
Institute of Design Aerodynamics
DLR, German Aerospace Center
D-38108, Lilienthalplatz 7, Braunschweig
Germany

ABSTRACT

The paper presents a design methodology for supersonic wing sections with hybrid laminar flow control. The approach is based on coupled Euler/boundary layer flow simulation and linear stability analysis for transition prediction. The investigations show that combinations of simple pressure distribution shapes can be used to optimize airfoils for maximum extent of laminar flow and hence minimum friction drag.

NOMENCLATURE

α	–	angle of attack
c_f	=	skin friction coefficient
c_l	=	lift coefficient
c_p	=	pressure coefficient
c_q	=	suction coefficient; $c_q=(V_s\,\rho)_w$
Ma	=	Mach number
Re	=	Reynolds number based on freestream condition
Φ_{LE}	=	Leading edge angle
N_{tr}	–	Transition N-factor (envelope method)

INTRODUCTION

Mission requirements of second generation supersonic civil transport (SCT) demand friction drag reduction which probably cannot be achieved with fully turbulent configurations. The technological potential of laminar control for SCT is up to now not entirely evaluated. Problems concerning suction rates or passive/active boundary layer control are at now subject of investigations. This is the context for the development of tools for, and the validation of, a laminar design methodology for SCT.

The aim of a laminar flow design is to move the region of the laminar/turbulent transition as far downstream as possible. In supersonic flow laminar control is only feasible using a combination of profile shaping and active laminar flow control. Appropriate measures could be air suction or wall cooling. High leading edge sweep angles in combination with blunt leading edges cause an enhancement of crossflow in the boundary layer in the leading edge region. Crossflow disturbances are amplified in this area and can provoke early transition. Particulary on the outer wing of supersonic aircrafts the leading edge is very thin. Hence it will be technically difficult to integrate suction panels in this area to control crossflow instability. To overcome this difficulties two possible solutions exists for the laminar design. First a sharp nose can be chosen as with the BCA-SST[1] concept. On such wedge shaped leading edges no crossflow disturbances are amplified in the nose region. But in high-lift conditions the flow separates at the leading edge. This generates additional vortex drag and may change the aircraft handling qualities. Another design option is to retain a blunt nose profile and to control the crossflow instabilities with an adequate leading edge shape. In both options Tollmien-Schlichting (TS) waves have to be damped with suction.

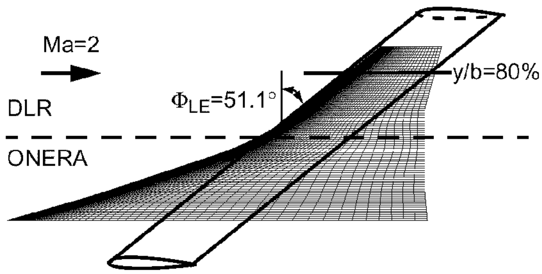

Fig. 1: Wing of the AS-1 configuration.

Since 1997 DLR and ONERA are cooperating in the supersonic laminar design with the goal to design and assess a three dimensional laminar wing. The investigations are carried out using the Aerospatiale AS-1 configuration for Ma=2 as a baseline wing shape. DLR investigates the outer wing with blunt supersonic leading edge. Similar investigations are performed by partner ONERA for the inner wing.

The investigation presented here is a qualitative and quantitative study of laminar airfoil design idealised as an infinite swept wing. As reference profile the wing section of the AS-1 configuration at 80% span is chosen (see **Fig. 1**).

Paper presented at the RTO AVT Symposium on "Active Control Technology for Enhanced Performance Operational Capabilities of Military Aircraft, Land Vehicles and Sea Vehicles", held in Braunschweig, Germany, 8-11 May 2000, and published in RTO MP-051.

1. DESIGN METHODOLOGY AND TOOLS

The laminar flow design methodology is based on a systematic study of different simple shaped pressure distributions with the goal to find the beneficial characteristics for laminarity. A combination of the most favorable distributions will yield the optimized laminar profile.

Starting from the reference airfoil new target pressure distributions are graphically defined and corresponding profile geometries are generated with an inverse design tool. After performing a laminar boundary layer computation and a stability computation the transition location can be determined with an assumed transition N-factor. Then a new boundary layer computation with known transition location provides the friction drag coefficient C_f.

1.1 Inverse design tool

According to **Fig. 2** the inverse design process starts with a graphic prescription of a target pressure distribution. Then an optimization loop starts. It consists of an optimizer EXTREM, the parametric profile generator PROFIX, the mesh generator MegaCads[7], the flow solver FLOWer[6] and the tool CPDIFF which calculates the object function for the optimizer by a summation of local c_p-differences between actual and target distribution.

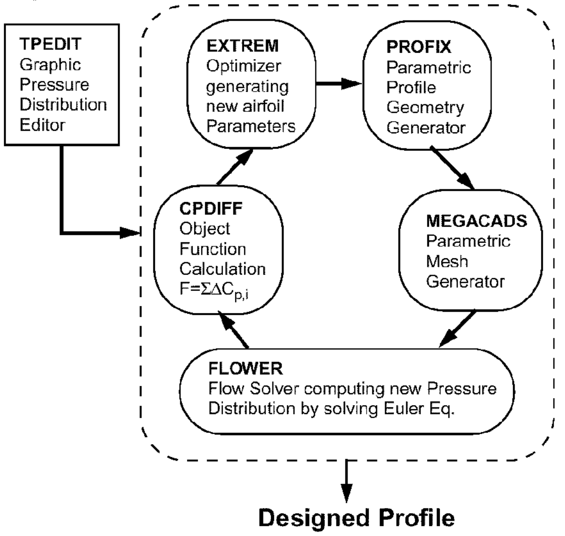

Fig. 2: Flowchart of the inverse design process.

The flow solver FLOWer

For the present application the FLOWer code solves the compressible three-dimensional Euler equations to provide the pressure distribution at each optimization step. This computation is performed on a grid of 122x20 cells. When the inverse design process stops a final Euler computation is achieved on a grid of 224x40 cells. This inviscid field solution is then used as the outer boundary condition for the boundary layer computation. As shown in **Fig. 3** an adequate residual convergence of the Euler computation is achieved after 54 iterations steps on the fine grid. The adopted convergence criterion for residual is 10^{-4}.

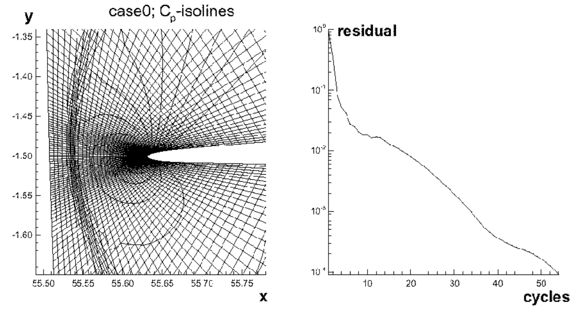

Fig. 3: Euler computation and convergence

The parametric profile generator PROFIX

This tool generates profiles by catenating geometric support points with Bezier curves. Each support point is defined by 3 parameters: the locations x, y and the local curve slope. To define a blunt nose a ramp function is used with a prescribed infinite slope at x/c=0. This tool uses the basic curve function routines introduced by H. Sobieczky[4]. **Fig. 4** sketches an example how the curve functions are used to define the airfoil.

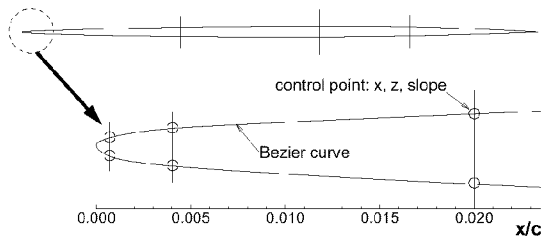

Fig. 4: Sketch of profile parametrization.

The number of support points can be changed by user input according to local profile shaping requirements. For the present application 14 support points are used which are controlled by 32 geometric parameters.

Performance of the inverse design tool

The location of the support points are chosen in a way to allow an accurate reproduction of the target pressure distribution. During the inverse design the angle of attack is a free parameter. **Fig. 5** shows the results of the design process after 12 optimization levels. The calculated profile has a pressure distribution in sufficient agreement to the graphically prescribed target pressure distribution.

For reason of structural constraints the profile thickness of the reference airfoil has to be retained. During the inverse design this is achieved by local adaption of the target pressure distribution.

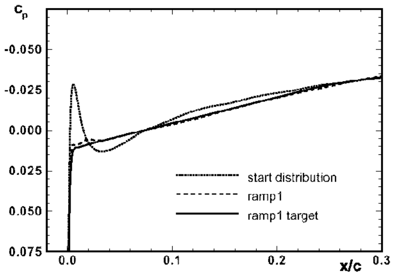

Fig. 5: Performance of the inverse design

Boundary-Layer Model

The code SOBOL[5] used here solves the second-order boundary-layer equations. Solution of this set of equations can be regarded as classical boundary-layer solutions corrected so that wall curvature, viscous interaction and wall-normal inviscid flow gradients are taken into account. The solution of the system of partial differential equation is performed with a space marching finite-difference method. The simulation of suction is implemented in the code. For the present design study a uniform suction panel with a suction power corresponding to a c_q=0.33 10^{-3} over a length of $\Delta x/c$=0.06 is selected. This suction power amount emerges from preliminary suction investigations.

Stability analysis

The code COAST[2] analyses the instability of compressible boundary layers with the semi-empirical e^N-method[3]. COAST solves the linear stability equations of compressible, parallel, three-dimensional flow along curved surfaces. The envelope N-factor integration method is implemented and used for the present application. Curvature effects are not considered. The transition N-factor for free flight conditions is assumed to be N_{tr}=6.

2. LAMINAR DESIGN

2.1 Investigated pressure distributions

Starting from the reference profile denoted by *case0*, three different series of generic pressure distributions were generated. The variation of the pressure distribution is restricted to the first 25% of chord. The first series denoted by *ramp* (**Fig. 6**) consists of a variation of the slopes of a linear pressure drop without suction peak. The second series denoted by *lev* shows a parallel pressure level shift of the linear pressure drop (**Fig. 7** top).

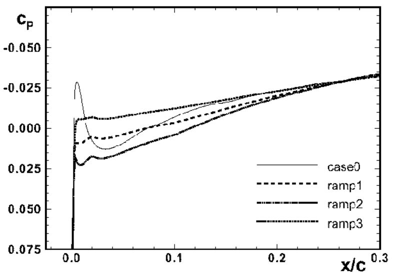

Fig. 6: Generic *ramp* pressure distributions.

The last series denoted by *top* combines three different suction peaks with a *ramp* distribution (**Fig. 7** bottom)

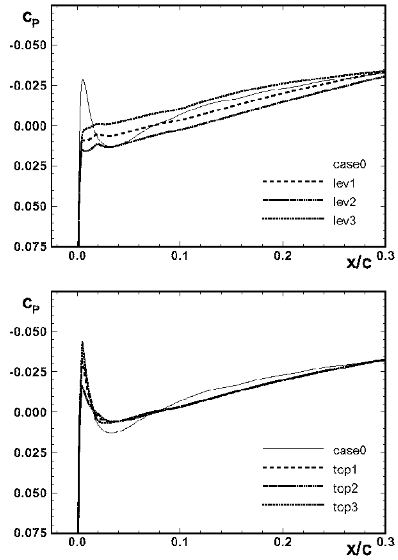

Fig. 7: Generic *lev* and *top* pressure distributions.

2.2 Investigation of suction models

Variation of suction panel position

The aim is to study the effect of the suction panel location on wave damping/amplification behavior. This is done by moving the suction panel with the same suction power up and downstream. This investigation is carried out on the *top1*-distribution. The stability situation without suction is shown in **Fig. 8**. Note that the stability relevant frequency are is 4kHz.

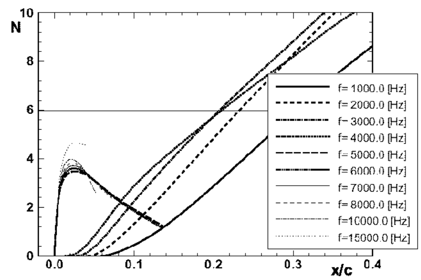

Fig. 8: Stability of case *top1* (no suction).

The first obvious suction approach is to begin suction at 19% chord in order to damp TS-waves around the estimated transition location. This trial fails as shown in **Fig. 9** (top). Here TS-waves are already too much amplified and this reduces the sensitivity of the waves to suction.

The following suction approach shifts the suction panel upstream. **Fig. 9** (bottom) shows an increase of the suction impact on the TS-wave amplification by the chosen upstream shift. The optimized suction location is found at 8.4% chord. Here suction is performed where the waves just begin to grow. The transition is located now at 36% chord.

This investigation shows the necessity, for the suction fitness evaluation to perform an optimization of the suction panel location. This is particulary important for pressure distributions with a distinct streamwise separation of crossflow waves from TS-waves.

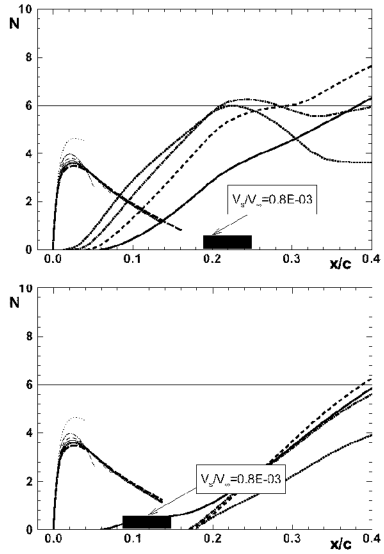

Fig. 9: Optimization of suction panel location.

Variation of suction panel extent

Here we vary the local suction coefficient by keeping the total suction power constant and the suction panel location unchanged at 5% chord. Three suction panel lengths are investigated on the *ramp1*-distribution whose natural stability is shown in **Fig. 10**. Note that the lack of the suction peak causes a distinct dominance of crossflow waves.

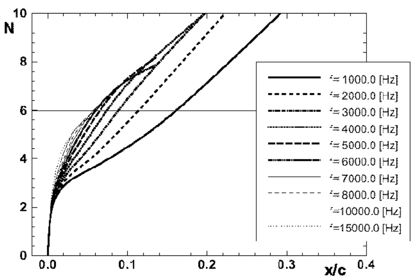

Fig. 10: Stability of the *ramp1*-distribution (no suction).

As given in **Fig. 11** increasing the suction length causes a dilution of the suction efficiency and so yields no better damping behavior on TS-waves. This instance meets the technical constraint which demand short suction panels.

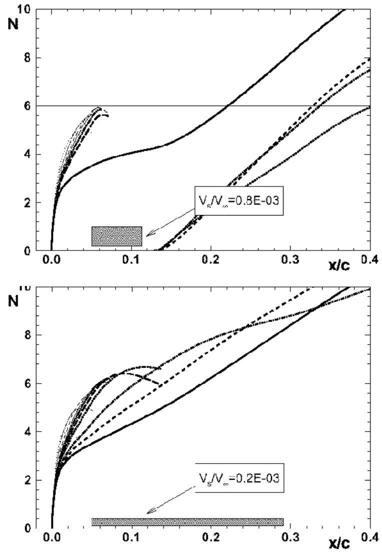

Fig. 11: Variation of the suction panel length

2.3 Design result

Laminarity with suction

All stability results shown here are optimized regarding the suction panel location according to 2.2. The most favorable *ramp* distribution is *ramp3* **Fig. 12** (top). Note that the lower slope of the pressure drop yields a longer laminar extent.

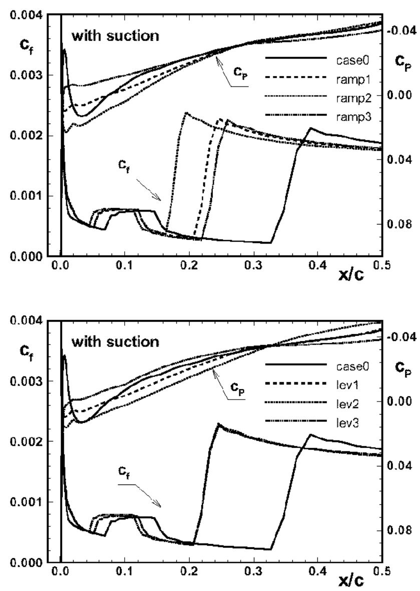

Fig. 12: Transition on *ramp* and *lev* distributions.

The transition location of the three *lev* distributions do not differ from each other (see **Fig. 12** bottom). This shows that the pressure level cannot be used as an effective design attribute. On this account the *lev* distributions are not considered for the further design.

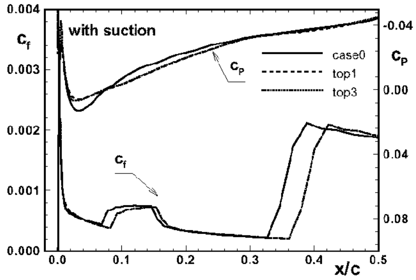

Fig. 13: Transition on the *top* distributions.

The *top1* and *top3* distribution have the same transition location at 36% chord (see **Fig. 13**) and so they represent the most favorable designs due to the property that suction peak damps crossflow disturbances.

Optimized design

Combining the characteristic shape of *top1* and *ramp3* a new pressure distribution is generated. With an optimized suction location the new designed profile has a laminar length of 46% chord, see **Fig. 14**.

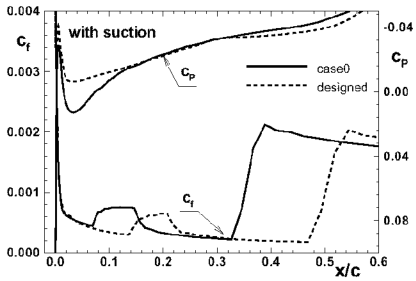

Fig. 14: Designed pressure distribution.

Fig. 15 illustrates the impact of the new pressure distribution on the stability. The higher suction peak has a damping effect on crossflow waves. The shorter pressure rise extent after the peak damps the TS-waves with a parallel shift of the N-curves downstream maintaining the effect of suction.

Table 1: Comparison of total drag

case	c_{dp}	c_{df}	$c_{dp}+2c_{df}$
case0 (no suction)	0.006828	0.001651	0.01013
case0 (suction)	0.006828	0.001280	0.009388
designed (suction)	0.006780	0.001039	0.008821

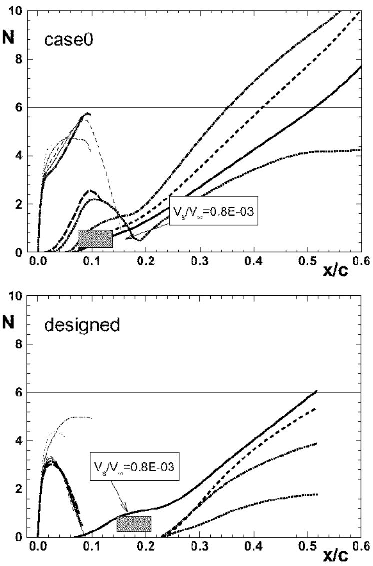

Fig. 15: Stability of the designed profile.

A comparison of both airfoil geometries in **Fig. 16** shows that the new designed profile has about the same curvature at the leading edge and the same thickness as the reference airfoil *case0.*

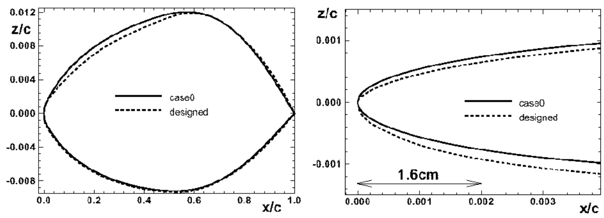

Fig. 16: Geometry of the designed profile.

Table 1 shows that with the new distribution the total drag can be reduced by about 5.9% compared with the reference distribution *case0*. In the third column the total airfoil drag of upper and lower surface was conservatively estimated by using twice the skin friction drag of the upper surface.

Reynolds number sensitivity

The aim is here to evaluate the spanwise range of the validity of laminar characteristics of the designed profile. This is done by increasing the Reynolds number about 1.5 times and decreasing 0.75 times with reference to the design Reynolds number of Re=4.8 $10^6[m^{-1}]$. This simulates a typical variation of the profile chord length.

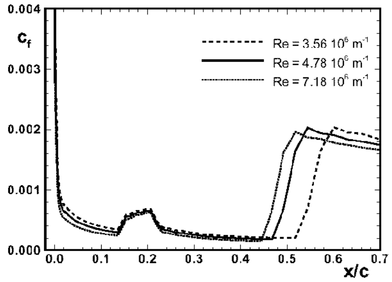

Fig. 17: Reynolds number sensitivity.

Fig. 17 shows the Reynolds number sensitivity of the designed profile. Transition location is not strongly affected by the given Reynolds number range. This indicates that the designed pressure distribution could be used over the whole outer wing of the AS-1.

Sensitivity to angle of attack

For the evaluation of the laminar pocket of the designed profile the angle of attack was changed in two directions by $\Delta\alpha$=0.3°. This causes an alteration of the lift coefficient of Δc_l=20%. The corresponding pressure distributions gives **Fig. 18**. The design angle of attack is α=2.02°

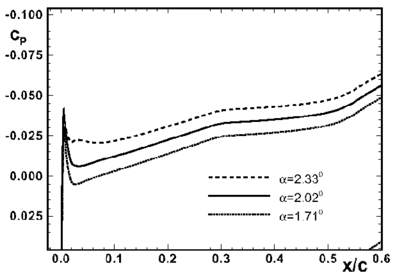

Fig. 18: Variation of the pressure distribution with the angle of attack.

The stability results in **Fig. 19** shows that the lower angle causes a negligible decrease of the laminar length of $\Delta x/c$=0.015. Increasing the angle of attack has a stronger impact. Here we have an amplification of crossflow waves due to the reduced suction peak and this causes a significant loss of laminar length shifting the transition location at about x/c=0.1.

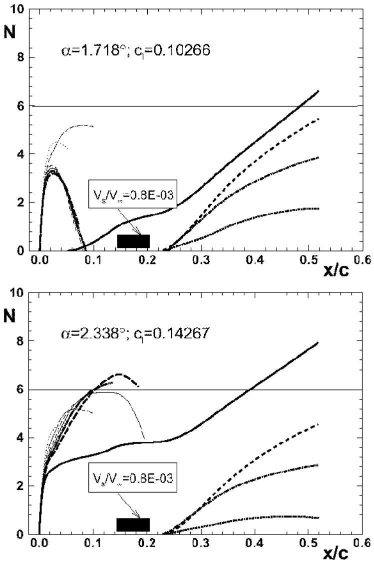

Fig. 19: Laminar pocket evaluation

3. CONCLUSION

The present work describes a successful design of laminar flow airfoils with a blunt supersonic leading edge. Simple shaped pressure distributions were generated and their stability analyzed. A combination of suction peak at leading edge to control crossflow and favorable pressure gradient after the peak to delay TS-instability were used to design an optimized pressure distribution for hybrid laminar flow control. The study shows that crossflow instability can be controlled only through profile shaping on a 51° swept wing with blunt leading edge at Ma=2. The location of a given suction panel was optimized to increase the efficiency of suction in order to enhance the extent of laminar flow. Compared to the turbulent reference design the new design has less wave drag and less skin friction drag, both for natural laminar flow and hybrid laminar flow control.

4. REFERENCES

[1] R.D. Wagner, m. C. Fischer, F.S. Collier, W. Pfenniger: "Supersonic Laminar Flow Control on Commercial Transports" ICAS-90-3.6.3

[2] Schrauf, G.: "COAST2 - A Compressible Stability Code, Users Guide and Tutorial". Report No. EF1-1973, 1993

[3] Arnal, D., "Boundary-Layer Transition: Prediction based on Linear Theory", *Special Course on Progress in Transition Modeling*, AGARD-R-793, Brussels, Belgium, 1993

[4] Sobieczky, H., Chourdhry, S., Eggers, T., "Parametrized supersonic transport configuration", 7th European Aerospace Conference (1994)

[5] Monnoyer, F., "Second Order BOundary Layers SOBOL Mk 2.7 Handbook", UVHC-LMF-001.

[6] Koll, N.; Rossow, C.C.; Becker, K.; Thiele, F., Megaflow A Numerical Flow Simulation System, Proceedings of the 21st ICAS Congress 1998, Melbourne.

[7] Brodersen, O.; Hepperle, M.; Ronzheimer, A.; Rossow, C.C.; Schöning, B., "The Parametric Grid Generation System MegaCads.",

Paper #3

Q by C. Ciray: What angle of attack was used in your calculations ? Did you try any value other than the design angle ?

A (A. Traore): The design angle of attack is 2.0 degrees. No, I investigated only the design angle.

This page has been deliberately left blank

Page intentionnellement blanche